Supporting Information

Thermally Activated Delayed Fluorescence Polymer Emitters with Tunable Emission from Yellow to Warm White Regulated by Triphenylamine Derivatives

Yuchao Liu,[a] *Guohua Xie,*[b] *Zhongjie Ren,*[a]* *and Shouke Yan*[a,c]*

[a] State Key Laboratory of Chemical Resource Engineering, College of Materials Science and Engineering, Beijing University of Chemical Technology, Beijing 100029, China.

[b] Hubei Collaborative Innovation Center for Advanced Organic Chemical Materials, Hubei Key Lab on Organic and Polymeric Optoelectronic Materials, Department of Chemistry, Wuhan University, Wuhan 430072, P. R. China.

[c] Key Laboratory of Rubber-Plastics, Ministry of Education, Qingdao University of Science & Technology, Qingdao 266042, P. R. China.

*E-mail: renzj@mail.buct.edu.cn (Ren, Z.); skyan@mail.buct.edu.cn (Yan, S.).

1. Experimental Procedures

1.1 Materials

All reactants were purchased from Adamas Reagent, Ltd. , Energy Chemiacl Co. Ltd., Merck KgaA, Heowns Co. Ltd. and J&K Scientific Ltd. without further purification and all solvents were supplied by Beijing Chemical Reagent Co. Ltd. Anhydrous and deoxygenated solvents were obtained by distillation over a sodium benzophenone complex.

1.2 Characterization

The NMR spectra were obtained using a Bruker AVANCE Ⅲ 400 spectrometer (400MHz). ^{1}H NMR and ^{13}C NMR were measured with TMS as internal standard. Electron spray mass spectra (ESI-MS) were collected on Xevo G2 Qtof using dichloromethane as the matrix. Elemental analyses were performed on a Vario EL cube. Gel permeation chromatography (GPC) analysis were carried out on a Waters 515-2410 system using polystyrene standards as molecular weight references and tetrahydrofuran (THF) as the eluent. Differential scanning calorimetry (DSC) was measured on a TA Q2000 differential scanning calorimeter at a heating rate of 10 ºC min^{-1} from 25 to 300 ºC and a cooling rate of 10 ºC min^{-1} from 300 to 25 ºC under nitrogen atmosphere. The glass transition temperature (T_g) was determined from the first cooling scan and second heating scan simultaneously. Thermogravimetric analysis (TGA) was performed with a METTLER TOLEDO TGA/DSC 1/1100SF instrument. The thermal stability of the samples was obtained by measuring their 5% weight loss while heating at a rate of 10 ºC min^{-1} from 25 to 800 ºC under a nitrogen atmosphere. Cyclic voltammetry (CV) was carried out in nitrogen-bubbled acetonitrile using CHI voltammetric analyser at room temperature. Tetrabutylammonium hexafluorophosphate ($TBAPF_6$ 0.1 M) was used as the electrolyte, and a glassy carbon working

electrode, a platinum wire auxiliary electrode, and an $Ag/AgNO_3$ pseudo-reference electrode were adopted in the conventional three-electrode system. Cyclic voltammograms were performed at scan rate of 100 mV s^{-1}. The onset potential was determined from the intersection of two tangents drawn at the rising and background current of the cyclic voltammogram. The oxidation and reduction behaviors of polymers were firstly determined in the $TBAPF_6$ acetonitrile solution and then ferrocene was added into the same solution as the internal reference to comfirm the potential values. The HOMO and LUMO energy levels were calculated according to the internal reference ferroceneredox couple in acetonitrile by using the following formulas (1)-(2):[1,2]

$$E_{HOMO} = -\left(E_{\left(onset,ox\ vs\ Fc^{+}/Fc\right)} + 5.1\right), \quad (1)$$

$$E_{LUMO} = -\left(E_{\left(onset,red\ vs\ Fc^{+}/Fc\right)} + 5.1\right). \quad (2)$$

UV/Vis absorption spectra were recorded on a Hitachi U-2910 spectrophotometer. PL spectra were recorded on a Hitachi F7000 fluorescence spectrophotometer. The temperature dependence of transient PL decay curves and PL spectra in vacuum or air were performed using FLS980 spectrometer from Edinburgh Instruments Limited. The photoluminance quantum yields of blend films were measured on FLS980 with an integrating sphere (φ = 150 mm) under air or nitrogen atmosphere. The prompt fluorescence (PF), and delayed fluorescence (DF) emission and radiative decay spectra were determinated using nanosecond gated luminescence and lifetime measurements with either a high-energy pulsed Nd:YAG laser emitting (EKSPLA) or a N2 laser emitting. The CIE coordinates were obtained using CIE1931xy.V.1.6.0.2 application program.

1.3 Molecular Simulation and Calculation

The following procedures were carried out to optimize the molecular structures, to depict the MOs distribution, to calculate the energy levels of excited state, and to analyze the natural transition orbital (NTO) of the polymers. Firstly, the 2D molecular structures of the polymers were designed using ChemBioDraw Ultra 12.0 software, and then the 3D structures of these polymers were optimized using ChemBio3D Ultra 12.0 by minimizing the energy of the molecule using the MM2 mode. The resulting structure was further optimized in Gaussian 09 (supported by Chemcloudcomputing of BUCT) by performing a density functional theory (DFT) calculation in the RB3LYP mode with a 6-31G (d, p) basis set in the ground state. According to the calculation results, the energy properties of these polymers in the excited state (singlet and triplet energy levels, highest occupied molecular orbital (HOMO) and lowest unoccupied molecular orbital (LUMO) levels, oscillator strength (*f*) and the electron density distributions in these levels) were determined using Gaussian 09 with RB3LYP/6-31G (d, p) in a time dependent (TD) mode. To boost the calculation precision of the singlet and triplet energy levels, the number of calculated states was set to 5. After the pretreatment of NTO analysis by Multiwfn 3.4, the NTO results of electron-hole orbital distributions are exported by GaussView 5.0.

1.4 Materials synthesis

Scheme S1. Synthesis route for PTDP-5 and PTDP-10.

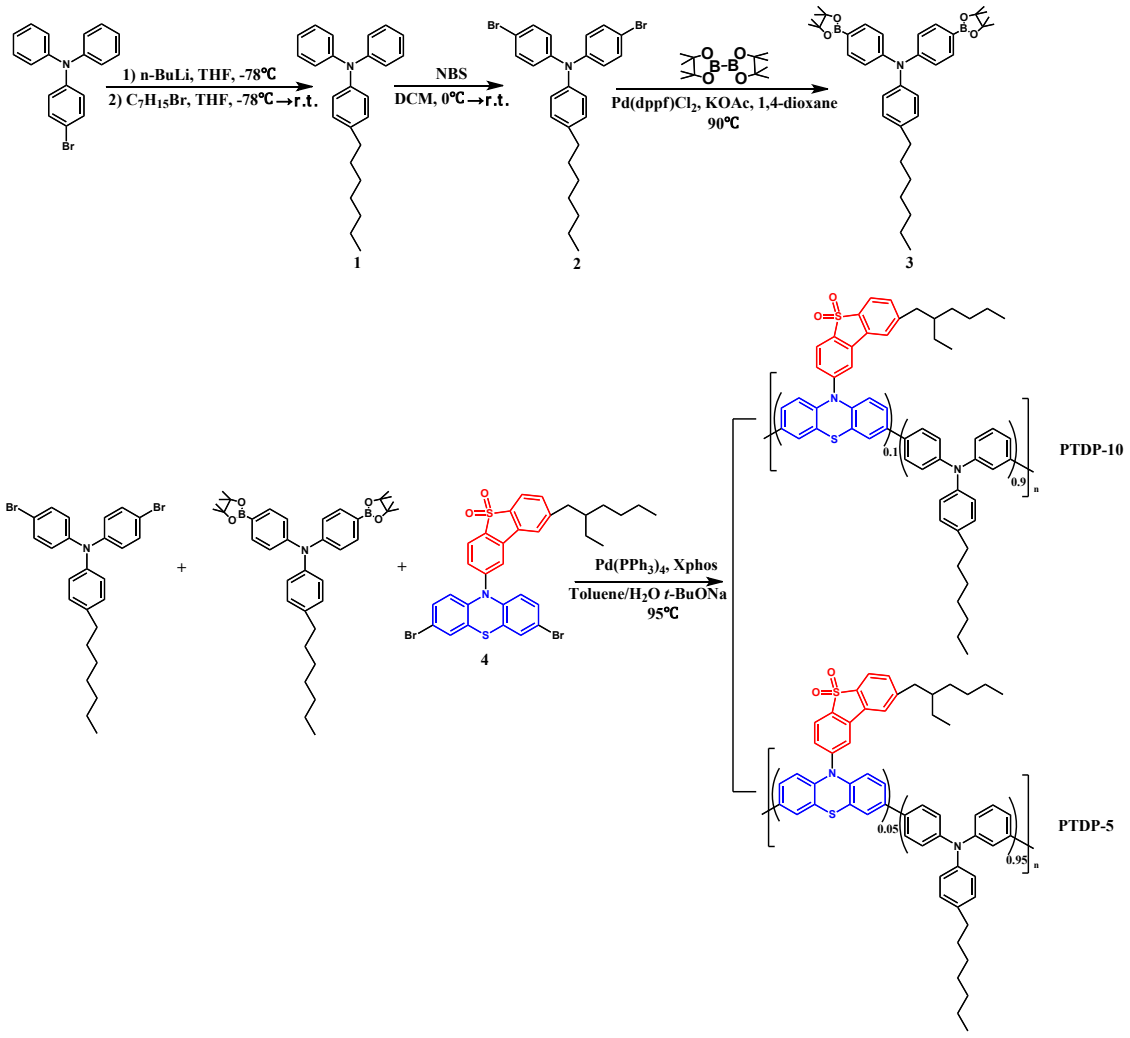

Synthesis of *N*-heptyl triphenylamine (TPA-C$_7$) (1): To a stirred solution of 4-bromotriphenylamine (6.48 g, 20 mmol) in dry tetrahydrofuran (100 mL) was dropped 14 mL n-BuLi dissolved in *n*-hexane (1.6 M) at -78 ºC within 30 min. After stirring for another 1 h at -78 ºC, the 1-bromo-heptane (3.8 g, 21 mmol, 1.05 eq) diluted by tetrahydrofuran (20 mL) was added slowly into the reaction mixture and stirred for further 5 h. The mixture was poured into abundant cold 5% HCl/water and extracted with dichloromethane. Then the organic was washed with water

and dried over anhydrous $MgSO_4$. After filtration and evaporation, the crude product was purified using silica gel chromatography (hexane: CH_2Cl_2 = 10:1), and then dried under vacuum to afford TPA-C_7 as colorless, viscous liquid (yield: 6.3 g, 93%).

^{1}H NMR (400 MHz, Acetone-d_6) δ 7.31-7.18 (m, 4H), 7.14 (d, *J* = 6.8 Hz, 2H), 7.08-6.89 (m, 8H), 2.64-2.50 (m, 2H), 1.70-1.53 (m, 2H), 1.43-1.21 (m, 8H), 0.92-0.78 (m, 3H).

^{13}C NMR (101 MHz, $CDCl_3$) δ 148.06, 145.35, 137.82, 129.17, 129.10, 124.72, 123.69, 122.23, 35.42, 31.84, 31.53, 29.37, 29.22, 22.71, 14.14.

MS [M+H]: 344.2379; calculated 343.23.

Synthesis of *N, N*-bis(4-bromophenyl)-4-heptyl benzenamine (TPA-C_7-Br) (2):

To a stirred solution of Cz-C_7 (5.15 g, 15 mmol) in dry dichloromethane (100 mL) was added *N*-bromosuccinimide (6.68 g, 37.5 mmol, 2.5 eq) dissolved in dry dichloromethane (50 mL) slowly at 0 ºC. The mixture was stirred for 24 h at room temperature under dark conditions. The reaction mixture was then poured into water, and extracted with dichloromethane. Then the organic was washed three times with water and dried over anhydrous $MgSO_4$. After filtration and evaporation, the crude product was purified using silica gel chromatography (hexane:CH_2Cl_2 = 10:1), and then dried under vacuum to afford TPA-C_7-Br as pale yellow liquid (yield: 6.74 g, 90%).

^{1}H NMR (400 MHz, $CDCl_3$) δ 7.35-7.29 (m, 4H), 7.11-7.05 (m, 2H), 6.99-6.94 (m, 2H), 6.94-6.88 (m, 4H), 2.61-2.52 (m, 2H), 1.67-1.48 (m, 4H), 1.44-1.21 (m, 6H), 0.98-0.83 (m, 3H).

^{13}C NMR (101 MHz, $CDCl_3$) δ 146.73, 144.39, 138.96, 138.90, 132.23, 129.50, 124.99, 114.98, 35.07, 33.61, 31.82, 31.46, 29.34, 22.67, 14.11.

MS [M+H]:499.05; calculated 500.568.

Synthesis of *N, N*-bis (4- (pinacolato)diboron)-4-heptyl benzenamine (TPA-C7-BPD) (3): A mixture of TPA-C_7-Br (2.50 g, 10 mmol), KOAc (5.9 g, 60 mmol, 6 eq), bis(pinacolato)diboron (7.6 g, 30 mmol, 3 eq), and dry 1,4-dioxane (100 mL) was stirred for 12 h at 90 ºC in argon atmosphere. The reaction mixture was poured into water and extracted with ethyl acetate. The organic layer was washed adequately with water and dried over anhydrous $MgSO_4$. After filtration and evaporation, the crude product was purified using silica gel chromatography (hexane: ethyl acetate = 10:1) to afford pale yellow liquid. Then the solid can be precipitated out after dropping the concentrated solution into cold hexane and dried under vacuum to afford TPA-C_7-BPD as yellow solid (yield: 5.20 g, 87%).

^{1}H NMR (400 MHz, $CDCl_3$) δ 7.70 (d, J = 8.4 Hz, 4H), 7.08 (td, J = 13.1, 8.4 Hz, 8H), 2.61 (dd, J = 13.4, 5.6 Hz, 2H), 1.64 (dt, J = 15.4, 7.5 Hz, 3H), 1.47-1.22 (m, 30H), 0.93 (ddd, J = 22.1, 15.0, 8.1 Hz, 4H).

^{13}C NMR (101 MHz, $CDCl_3$) δ 149.24, 143.47, 137.89, 134.80, 128.31, 124.80, 121.36, 82.54, 34.08, 32.56, 30.79, 30.40, 28.32, 28.15, 23.84, 21.41, 12.95.

MS [M+H]:596.4114; calculated 595.41.

Synthesis of 2-ethylhexyl-8-(3,7-dibromo-phenothiazin) dibenzothiophene-*S, S*-dioxide (DBSOR-PTZ-Br) (4) was synthesized according to the literature methods.[3]

2. Results and Discussion

Table S1. The results of organic elemental analyses.

Name	N[%]	C [%]	H [%]	S [%]	**Guest/Host**	**Guest%**
PTDP-10	3.87	82.49	7.08	1.81	TADF：TPA=1:8.77	10.24%
PTDP-5	2.70	84.20	8.99	0.74	TADF：TPA=1:16.58	5.70%

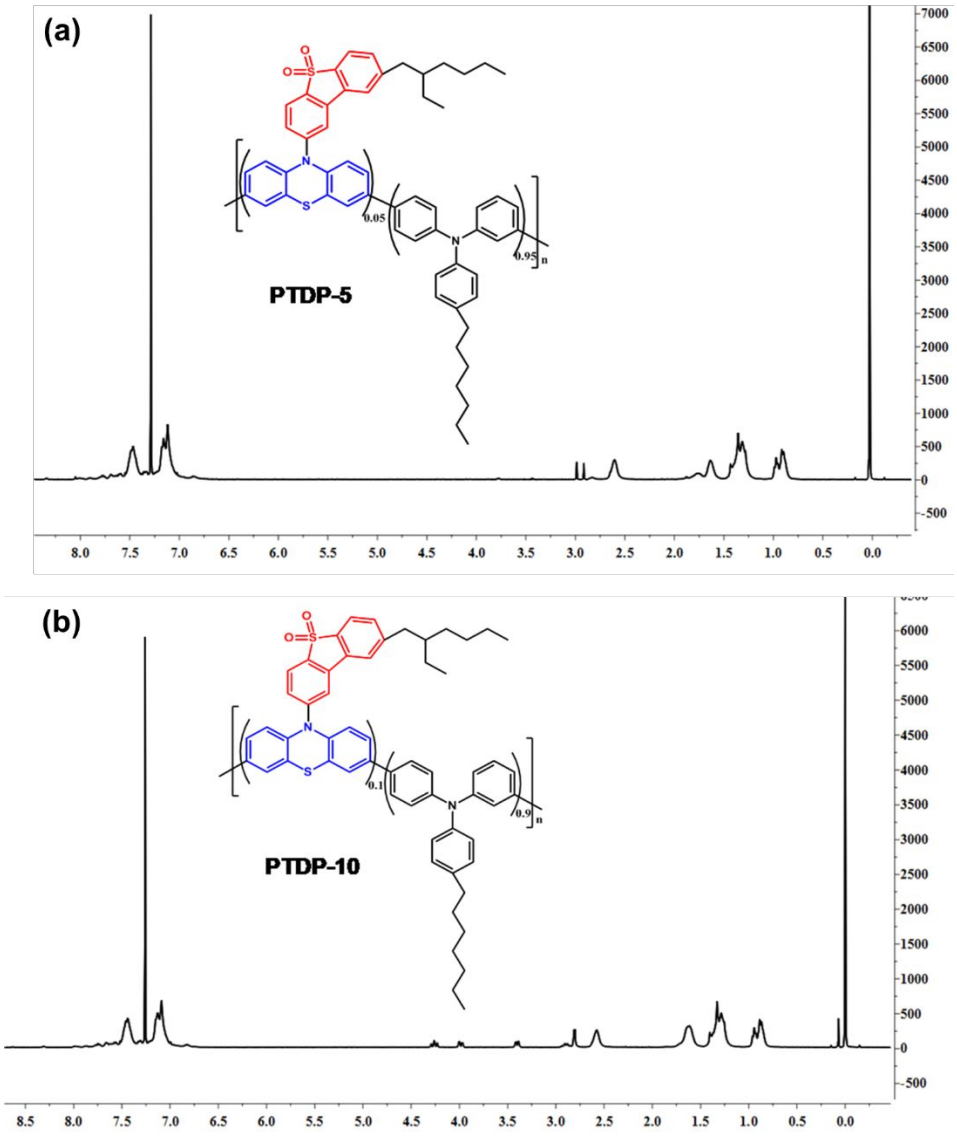

Figure S1. ^{1}H NMR spectroscopies of (a) PTDP-5, (b) PTDP-10.

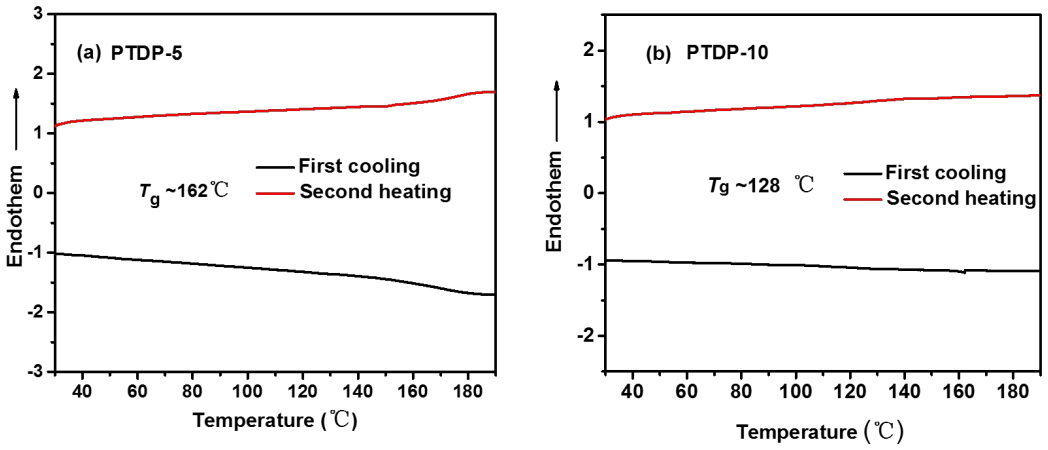

Figure S2. DSC thermograms of (a) PTDP-5, (b) PTDP-10 on the first-cooling and second-heating processes at a scanning rate of 10 ºC min^{-1} under N_2.

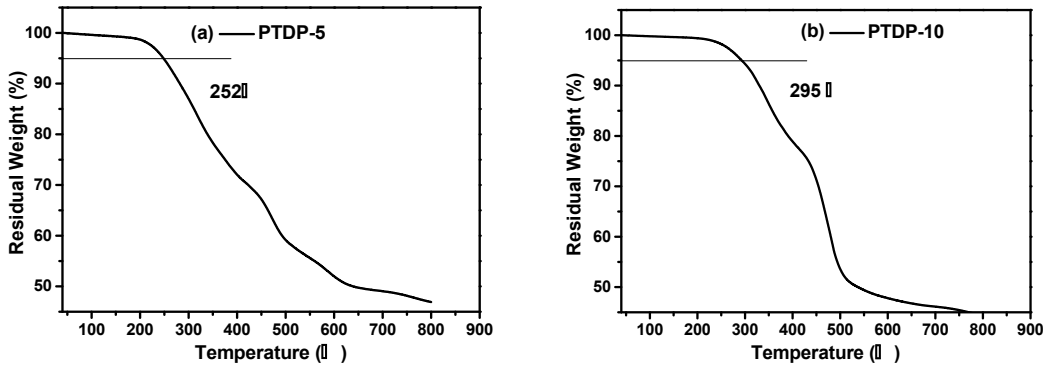

Figure S3. TGA curves of (a) PTDP-5, (b) PTDP-10 at a heating rate of 10 ºC min^{-1} under N_2.

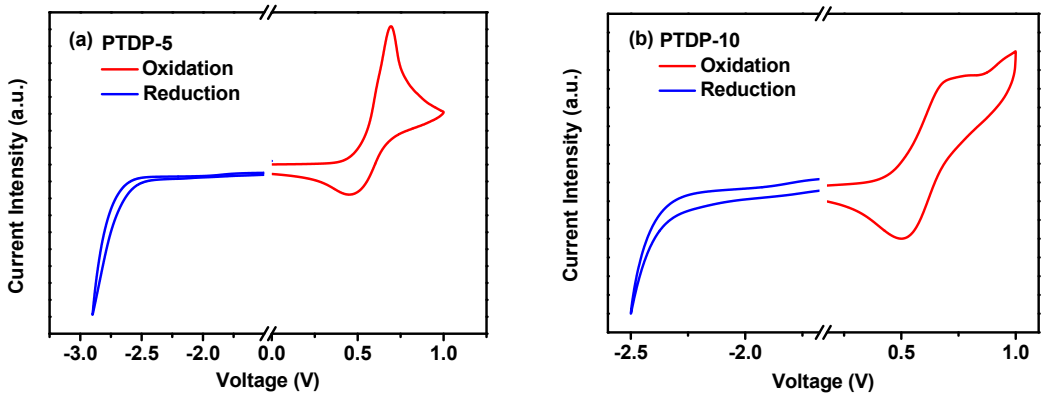

Figure S4. Cyclic voltammograms of (a) PTDP-5, (b) PTDP-10 obtained in the degassed anhydrous acetonitrile solution.

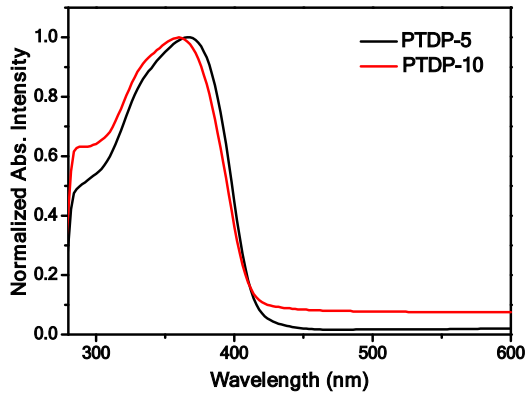

Figure S5. UV-vis absorption of the polymeric dilute solution in toluene.

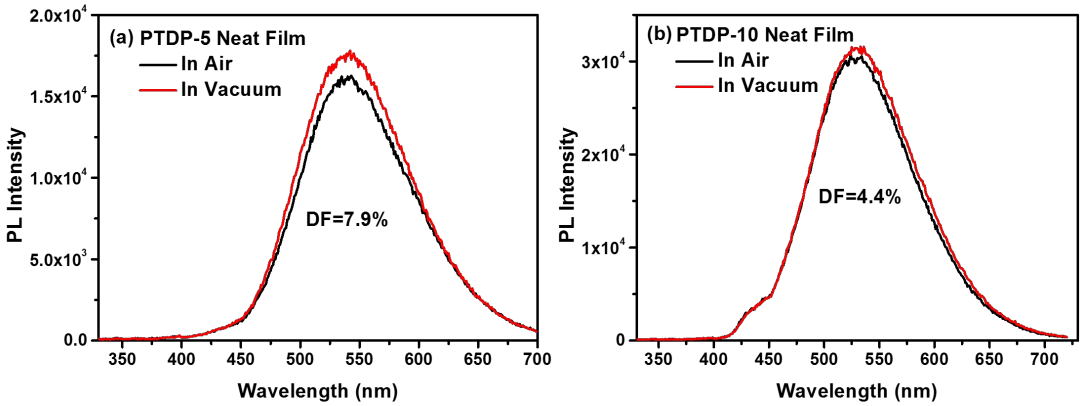

Figure S6. Steady state fluorescence spectra of (a) PTDP-5, (b) PTDP-10-50 in neat film at room temperature. The proportions of delay fluorescence are shown in graphs.

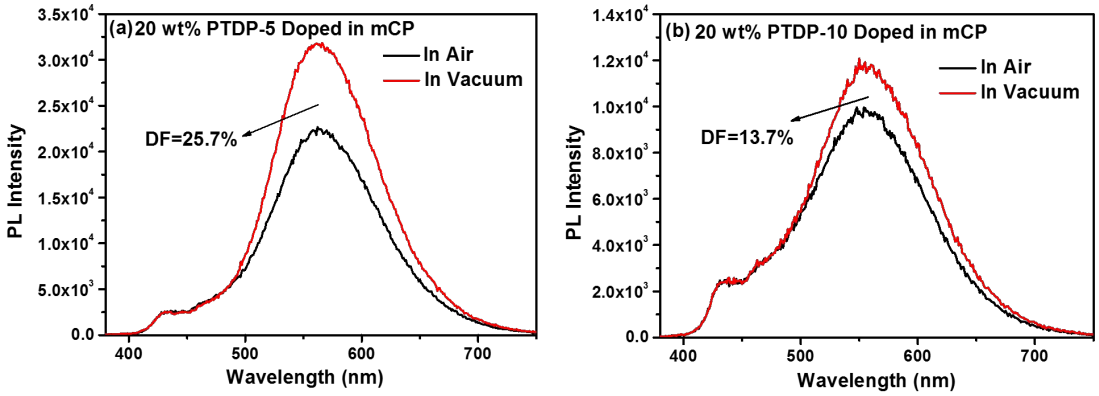

Figure S7. Steady state fluorescence spectra of (a) PTDP-5, (b) PTDP-10-50 doped in mCP film at room temperature. The proportions of delay fluorescence are shown in graphs.

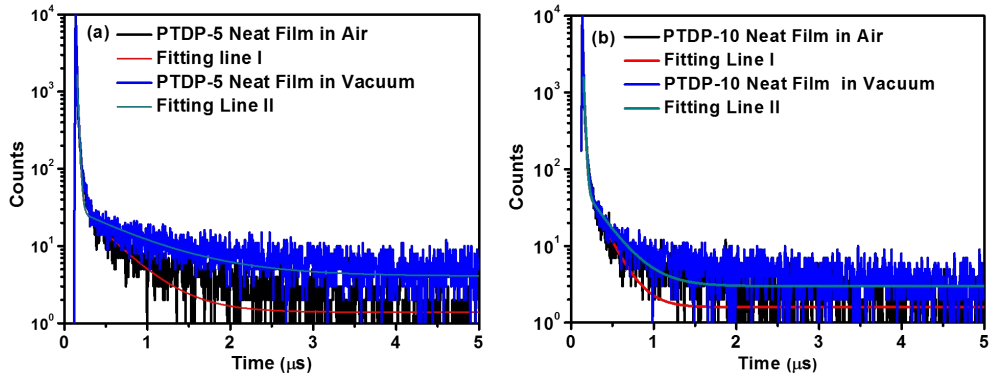

Figure S8. Transient PL decay characteristics of (a)PTDP-5, and (b) PTDP-10 in neat film at room temperature. Black curves and corresponding fitting line are measured with O_2; the blue curves and corresponding fitting line are measured without O_2.

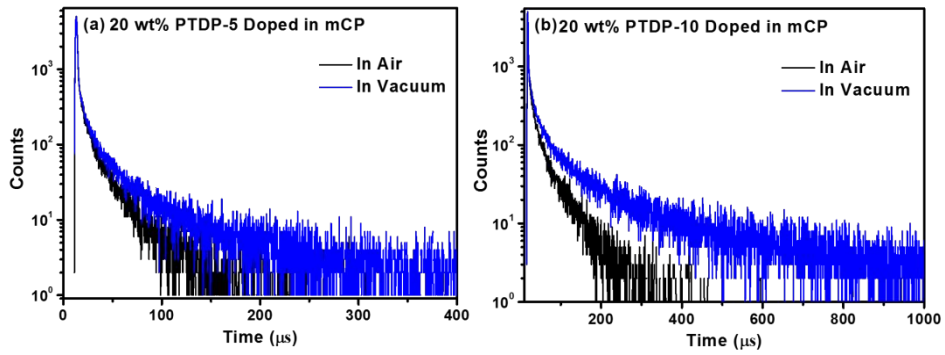

Figure S9. Transient PL decay characteristics of (a)PTDP-5, and (b) PTDP-10 in mCP doped film at room temperature. Black curves and corresponding fitting line are measured with O_2; the blue curves and corresponding fitting line are measured without O_2.

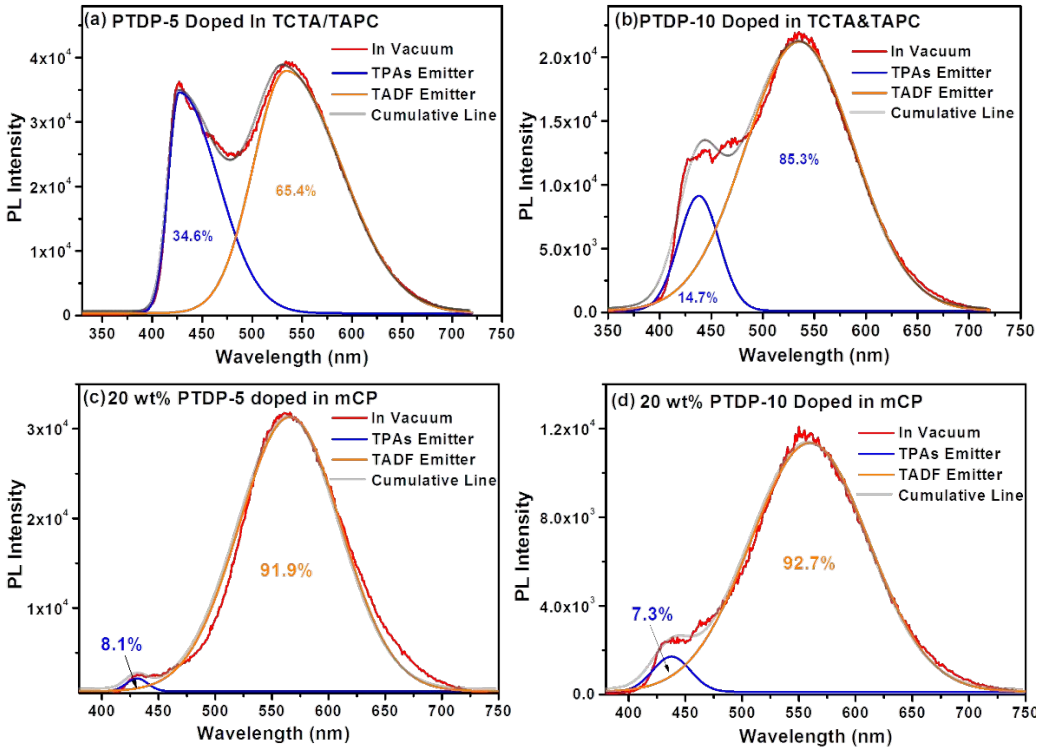

Figure S10. The multiple peak fitting results of doped emitters: (a) 10 wt% PTDP-5 doped in TCTA&TAPC; (b) 10 wt% PTDP-10 doped in TCTA&TAPC; (c) 20 wt% PTDP-5 doped in mCP; (d) 20 wt% PTDP-10 doped in PTDP-10 doped in mCP.

Table S2. Photophysical Properties of the Blend Film.

Emitter	$\emptyset_{PL}^{TADF}$ [%][a]	τ_p/ratio [ns]/[%][b]	τ_d/ratio [μs]/[%][c]	k_p [10^7 s^{-1}][d]	k_d [10^3 s^{-1}][e]	k_{ISC} [10^7][f]	k_{RISC} [10^3][g]
PTDP-5 in TCTA&TAPC	65.4±0.5	14.7/31.3	283.4/34.1	2.1	1.2	3.5	7.3
PTDP-10 in TCTA&TAPC	85.3±0.2	30.1/47.7	325.6/37.6	1.6	1.1	1.5	5.4
PTDP-5 in mCP	68.6±0.4	20.1/42.9	115.3/25.7	2.1	2.2	1.8	13.8
PTDP-10 in mCP	54.4±0.2	24.5/40.7	173.4/13.7	1.7	0.8	1.0	7.7

[a]The isolated PLQY values of TADF emitter. These values can be calculated by the equation: $\emptyset_{PL}^{TADF} = \emptyset_{PL}^{total}\frac{S_{TADF\ emitter}}{S_{total\ emitter}} = \emptyset_{DF}^{TADF} + \emptyset_{PF}^{TADF}$ (3), where $\emptyset_{PL}^{total}$ is the total PLQY values comprised by TPAs blue emitting and TADF orange-yellow emitting. The $S_{TADF\ emitter}$ and $S_{total\ emitter}$ are curvilinear integral areas of TADF emitting and total emitting, respectively, from the **Figure S10**. [b]The lifetime and the ratio of the prompt fluorescence ($\emptyset_{PF}^{TADF}$) measured in blend film without O_2. [c]The lifetime and the ratio of the delayed fluorescence ($\emptyset_{DF}^{TADF}$) measured in blend film without O_2. [d]The prompt fluorescent emission rates constants (k_p), which can be obtained by the equation: $k_p = \emptyset_{PF}^{TADF}/\tau_p$, where the $\emptyset_{PF}^{TADF}$ value can be calculated by equation of $\emptyset_{PL}^{TADF} = \emptyset_{DF}^{TADF} + \emptyset_{PF}^{TADF}$ (4). [e]The delayed fluorescent emission rates constants (k_d), which can be obtained by the equation: $k_d = \emptyset_{DF}^{TADF}/\tau_d$ (5), where the $\emptyset_{DF}^{TADF}$ value can be obtained steady-state PL spectra, from **Figure 2** b&c and **Figure S7**. [f]The intersystem crossing (ISC) rate constant (k_{ISC}), calculated by the equation of $k_{ISC} = \frac{\emptyset_d}{\emptyset_{PL}\tau_p}$ (6). [g]The RISC rate constant (k_{RISC}), calculated by the equation of $k_{RISC} = \frac{\emptyset_d}{k_{ISC}\tau_d\tau_p\emptyset_{PF}}$ (7).

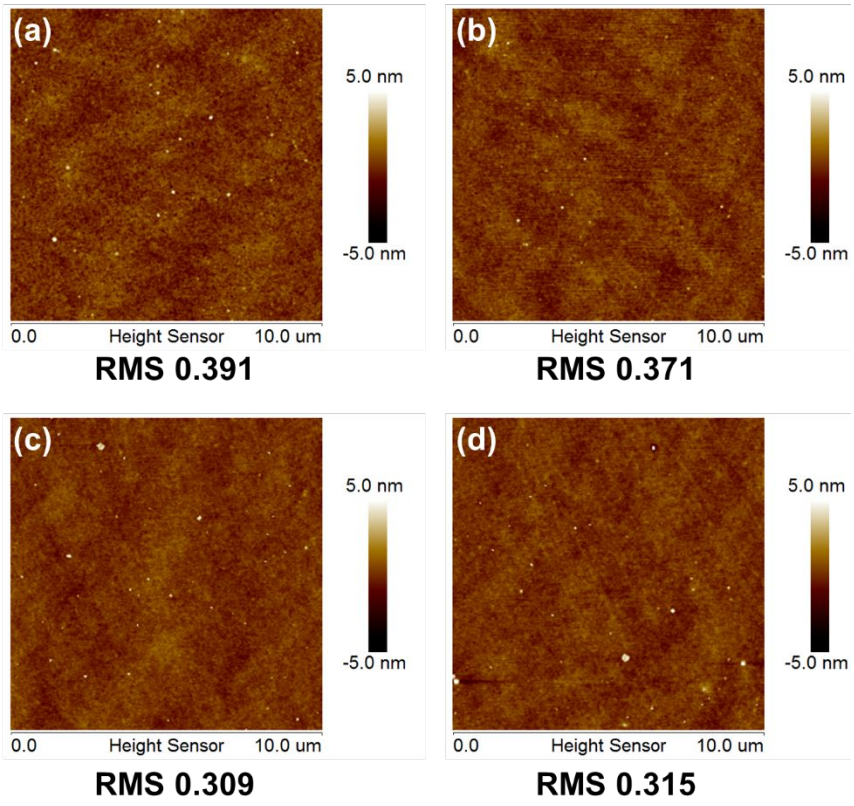

Figure S11. AFM height images and the RMS values of the spin-coated films: (a) PTDP-5 neat film; (b) PTDP-5: TCTA: TAPC (10:65:25 wt.%) blended film; (c) PTDP-10 neat film; (d) PTDP-10: TCTA: TAPC (10:65:25 wt.%) blended film. RMS values of the whole scanning area are shown below the images.

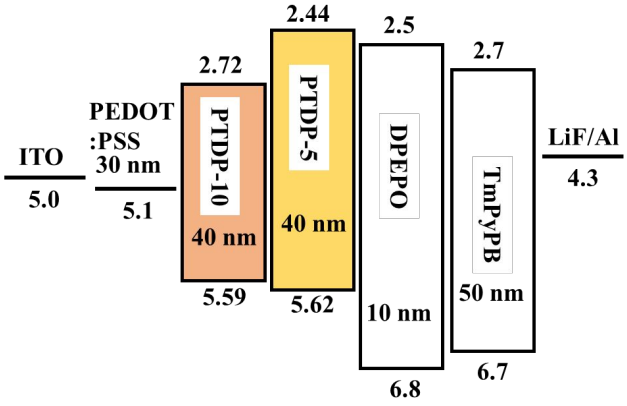

Figure S12. Structures of the nondoped devices and the corresponding energy level diagram with the HOMO/LUMO levels.

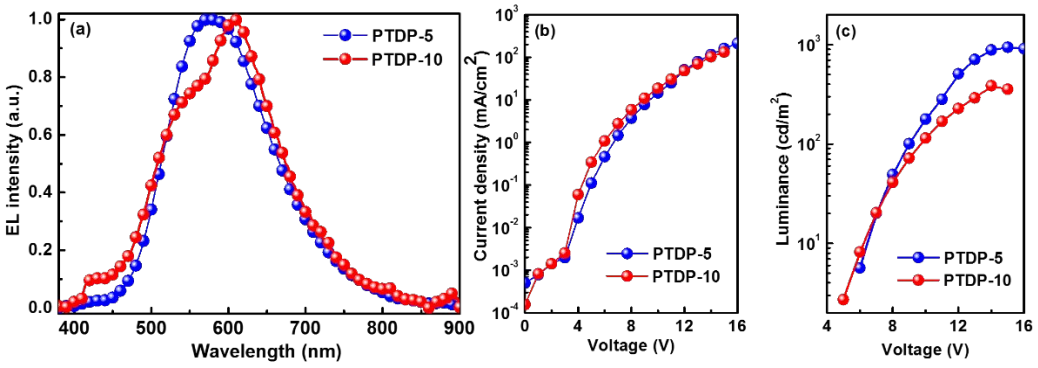

Figure S13. The device performances of PTDP-5 and PTDP-10 neat film as emitting layer. (a) The normalized EL spectra; (b) Current density-voltage-luminance curves; (c) Luminance-voltage curves.

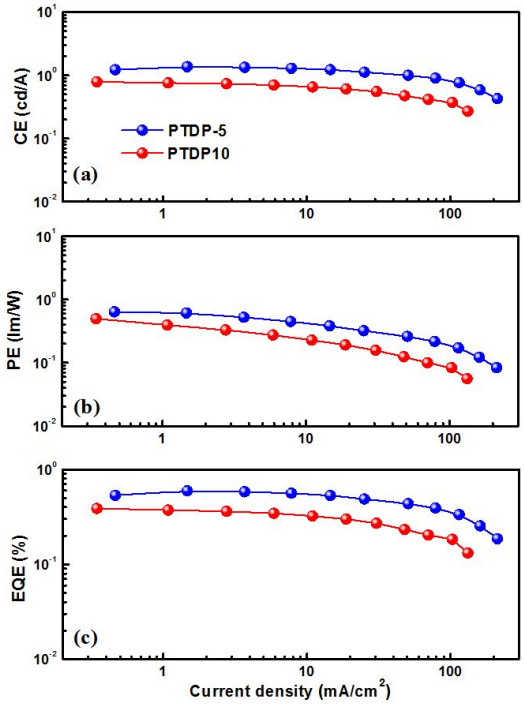

Figure S14. The nondoped device efficiency of PTDP-5 and PTDP-10 neat film as emitting layer. (a) Current efficiency-current density curves; (b) Power efficiency-current density curves; (c) External quantum efficiency versus luminance curves of the nondoped devices.

Table S3. The performances of nondoped devices.

Nondoped Emitter[a]	λ_{EL} [nm][b]	V_{on} [V][c]	L_{max} [cd m^{-2}][d]	CE_{max} [cd A^{-1}][e]	PE_{max} [lm W^{-1}][f]	EQE_{max} [%][g]
PTDP-5	576	4.9	978	1.5	0.6	0.6
PTDP-10	610	4.2	385	0.8	0.5	0.4

[a]The neat film of PTDP-5 or PTDP-10 acts as emitting layer. [b]The maximum electronluminance peaks. [c]The turn-on voltage at 1 cd m^{-2}. [d]The maximum luminance. [e]The maximum current efficiency. [f]The maximum power efficiency. [g]The maximum external quantum efficiency.

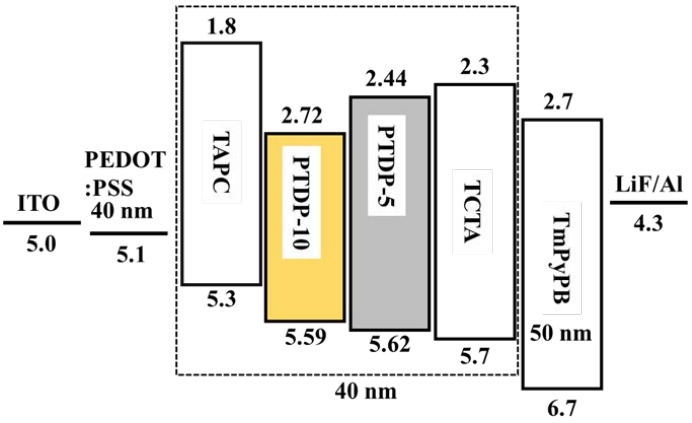

Figure S15. Structures of the doped devices and the corresponding energy level diagram with the HOMO/LUMO levels.

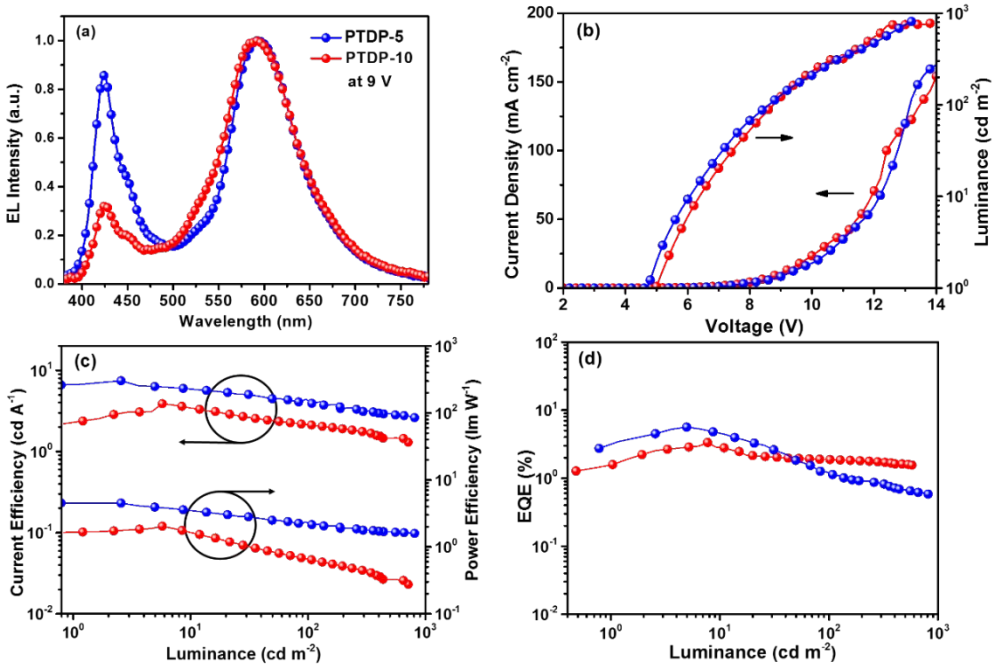

Figure S16. The device performances of PTDP-5 and PTDP-10 doped in TCTA&TAPC as emitting layer. (a) The normalized EL spectra at 9 V; (b) Current density-voltage-luminance curves; (c) Current efficiency-luminance-power efficiency curves; (d) External quantum efficiency versus luminance curves of the devices.

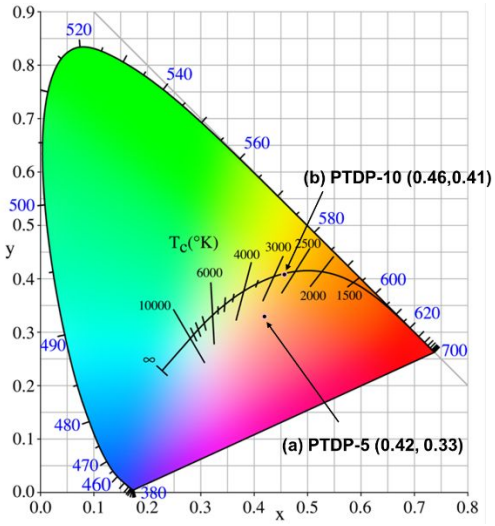

Figure S17. Commission Internationale de l'Eclairage (CIE) coordinates of (a) PTDP-5, (b) PTDP-10 doped in TCTA&TAPC as emitting layer.

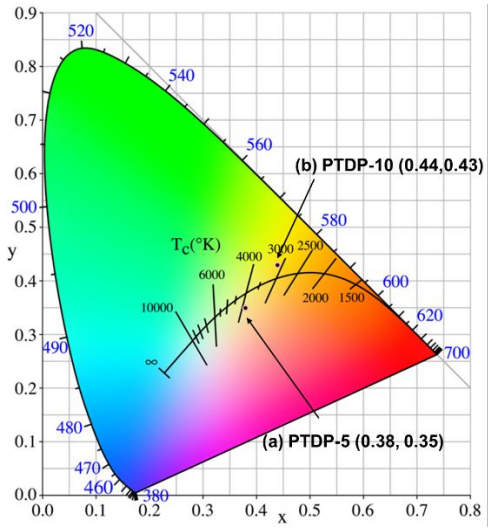

Figure S18. Commission Internationale de l'Eclairage (CIE) coordinates of (a) PTDP-5, (b) PTDP-10 doped in mCP as emitting layer.

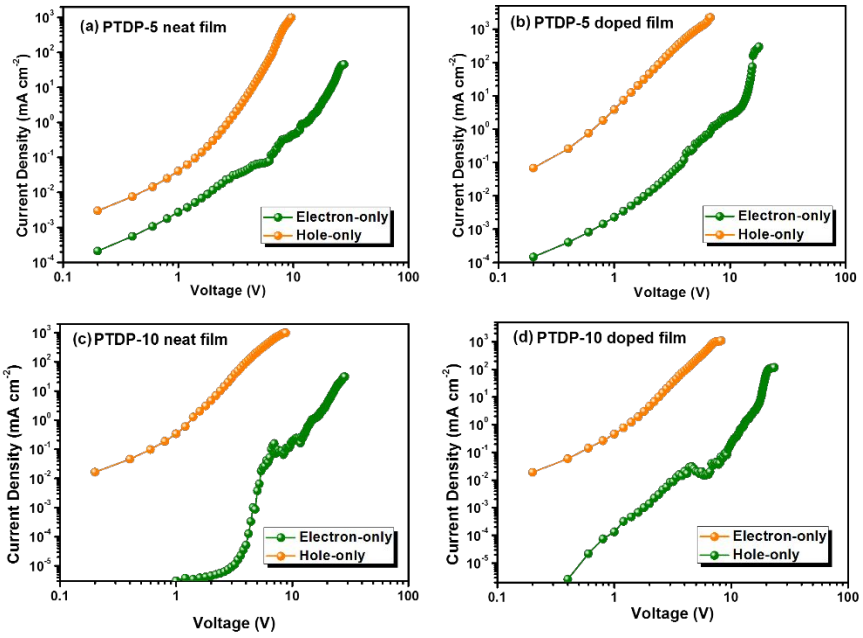

Figure S19. The current density-voltage curves of single carrier device. (a) PTDP-5 nondoped polymeric EML; (b) PTDP-5 doped polymeric EML; (c) PTDP-10 nondoped polymeric EML; (d) PTDP-10 doped polymeric EML.

Reference

(1) Bredas, J.-L. Mind the Gap! *Mater. Horiz.* **2014**, *1*, 17-19.

(2) Dias, F. B. Kinetics of Thermal-assisted Delayed Fluorescence in Blue Organic Emitters with Large Singlet–triplet Energy Gap. *Philos. Trans. R. Soc. A* **2015**, *373*, 20140447.

(3) Liu, Y., Wang, Y., Li, C., Ren, Z., Ma, D., Yan, S. Efficient Thermally Activated Delayed Fluorescence Conjugated Polymeric Emitters with Tunable Nature of Excited States Regulated via Carbazole Derivatives for Solution-Processed OLEDs. *Macromolecules* **2018**, *51*, 4615-4623.